

## Performance of oligomer 4-vinylpiperidine as a carbon dioxide corrosion inhibitor of mild steel

I. Ilim<sup>1,2\*</sup>, S. Bahri<sup>1,2</sup>, W. Simanjuntak<sup>2</sup>, Y.M. Syah<sup>1</sup>, B. Bundjali<sup>1</sup>, B. Buchari<sup>1</sup>

1. Department of Chemistry Faculty of Mathematic and Natural Science, Institut Teknologi Bandung, Jl. Ganesha No 10 Bandung, West Java, Indonesia

2. Department of Chemistry Faculty of Mathematic and Natural Science, The University of Lampung, Jl. S. Brojonegoro No 1 Bandarlampung, 35145 Indonesia

Received 17 Nov 2016,  
Revised 10 Mar 2017,  
Accepted 11 Mar 2017

### Keywords

- ✓ Oligomer;
- ✓ 4-vinylpiperidine;
- ✓ Corrosion rate;
- ✓ CO<sub>2</sub> corrosion;
- ✓ Corrosion Inhibitor

I.Ilim  
[ilim\\_ds@yahoo.com.au](mailto:ilim_ds@yahoo.com.au) or  
[ilim@fmipa.unila.ac.id](mailto:ilim@fmipa.unila.ac.id)  
+62 81379510280

### Abstract

Oligomer of 4-vinylpiperidine, O(4-VPP), synthesized by hydrogenation of oligomer 4-vinylpyridine, O(4-VP), was tested as a corrosion inhibitor to protect mild steel in brine solution saturated by carbon dioxide (CO<sub>2</sub>). Weight loss (wheel test), electrochemical impedance spectroscopy (EIS), and linear polarization (LP) measurements were used to determine the corrosion rates and the efficacies of the synthesized O(4-VPP). Weight loss experiments were carried out at temperature of 50 °C, in two different conditions, i.e without and with kerosene addition, while the other two techniques were applied only in brine solution without kerosene. Weight loss experiments demonstrated that the % protections of the synthesized inhibitor with the concentration of 10 mg L<sup>-1</sup> are 62.7±9.9 % in the absence of kerosene, and 58.1±1.6 % in the presence of kerosene. Based on the significant test, % protections of O(4-VPP) in brine solution with and without kerosene are not significantly different. EIS experiments were carried out at fixed temperature of 70 °C, and the results indicate that addition of 1 mg L<sup>-1</sup> of O(4-VPP) to brine solution led to increased charge transfer (R<sub>ct</sub>) from 21.8 Ω cm<sup>2</sup> to 49.9 Ω cm<sup>2</sup>, and with addition of 2 mg L<sup>-1</sup> led to increased R<sub>ct</sub> up to 90.9 Ω cm<sup>2</sup>, confirming the ability of the inhibitor to significantly decrease the corrosion rate of the mild steel investigated. To assess the effect of temperatures, the LP experiments were run at different temperatures of 30, 50, and 70 °C in the concentration range of inhibitor from 0 to 20 mg L<sup>-1</sup>. The results demonstrated that the higher the temperature and concentration, the higher the protection exhibited by the inhibitor suggesting that the inhibitor of O(4-VPP) was adsorbed onto surface of the mild steel through chemisorption supported by the adsorption thermodynamic parameters.

## 1. Introduction

Corrosion of pipelines (mild steel) used in the oil and gas industry during mining process due to the presence of CO<sub>2</sub> gas has been acknowledged as a serious problem for long time. This gas is known to react with water to produce corrosive carbonic acid which corrodes the inside surface of the pipelines [1,2]. It was reported that carbonic acid is more aggressive than hydrochloric acid at the same pH [3], and for this reason CO<sub>2</sub> corrosion has been a recognized problem in oil and gas production and transportation facility for many years [4-6]. Corrosion on the outer surface of the pipeline can be overcome by coating and /or cathodic protection, while the inner surface can be controlled by the addition of corrosion inhibitors. The use of corrosion inhibitors is an effective method for controlling acid corrosion including carbon dioxide corrosion [7-9] and the development of new corrosion inhibitors remains the focus of investigations. Various chemicals have been used for protection of metals against corrosion by carbon dioxide [9-20]. The use of polymer or oligomer of 4-vinylpyridine as corrosion inhibitor of various metals in various media has been reported in previous studies [20-26]. Ilim et al [20] reported that oligomer of 4-vinylpyridine, O(4-VP), protected the mild steel from carbon dioxide corrosion effectively, while the monomer 4-vinylpyridine promoted the corrosion. Because of its saturated molecular structure and its basic strength, oligomer of 4-vinylpiperidine, O(4-VPP) is presumed as a good corrosion inhibitor, and for this reason, the present study focuses on the use of O(4-VPP) for protection of mild steel from carbon dioxide corrosion. O(4-VPP) is not available commercially and data relating to this compound was not readily available, so the O(4-VPP) was synthesized by hydrogenation of O(4-VP). The oligomer product was

tested as corrosion inhibitor of mild steel in brine solution saturated carbon dioxide with / without kerosene. Weight loss and electrochemical methods were used to determine the effectiveness of O(4-VPP) as a corrosion inhibitor.

## 2. Experimental details

### 2.1. Materials and Apparatus

Materials used were 4-vinylpyridine (AR) from Merck, methanol (AR) from Merck, milli-Q water produced in our laboratory, H<sub>2</sub>O<sub>2</sub> (AR) from Merck, platinum oxide (AR) from Merck, glacial acetic acid (AR) from Merck, NaCl (AR) from Merck, NaHCO<sub>3</sub> (AR) from Merck, and food grade CO<sub>2</sub> gas from local supplier. Laboratory instruments used were rotary evaporator, Heidolph rotator, balance/ weighting, wheel oven manufactured by Detailed Design, Texas, Pine Model MSR electrode rotator, digital hot plate, EG&G Model 5210 Lock-in Amplifier and 273A Potentiostat controlled by EG&G Model 398 Electrochemical Impedance Software, Version 1.26, EG&G Princeton Applied Research Model 273A Potentiostat and EG&G Model 314 Multiplexer.

### 2.2 Preparation of solutions

Brines solution 3 % (w/v) as a corrosion electrolyte was prepared by dissolving 30 g NaCl and 100 mg NaHCO<sub>3</sub> in 1 L milli-Q water. To saturate the electrolyte with CO<sub>2</sub> gas, the gas was purged into the electrolyte at a rate of approximately 150–200 mL min<sup>-1</sup> and atmospheric pressure. Inhibitor solution with the concentration of 10,000 mg L<sup>-1</sup> in ethanol was freshly prepared prior to corrosion inhibition experiments.

### 2.3 Preparation of testing sample

Mild steels (coupon and cylindrical electrode) used in this experiment were SAE/AISI Grade 1022 according to AS 1443. According to spectrographic analysis, the sample contain 98.87% Fe and a series of minor components with varied amounts, include C (0.22%), Mn (0.74 %), Si (0.02 %), S (0.014 %), P (0.02 %), Ni (0.05 %), Cr (0.04 %), Mo (<0.01 %), Cu (<0.01 %), Al (<0.01 %). For weight loss experiment, a coupons (2 x 1 x 0.1) cm was prepared by sand blasting a sheet of mild steel with garnet (size 0.89 mm) and cut to size using a guillotine. Before use, the coupon was degreased by immersing in ethanol and then sonicated for two minutes, and then dried. The dimension and the weight of the sample were accurately measured using micrometer and four-digit analytical balance respectively. A mild steel cylinder electrode with the surface area of 3.02 cm<sup>2</sup>, to be used as a working electrode in linear polarization measurements, was polished with silicon carbide paper of grade 360, 400, 600 and 800 on a Heidolph rotator (rotated at 750 rpm), using ethanol as a lubricant.

### 2.4 Synthesis of O(4-VP)

A reaction mixture was prepared by mixing 50 g (0.48 mol), 4-vinylpyridine as monomer, 125 mL methanol 125 mL water, and 37.40 mL (0.33 mol) H<sub>2</sub>O<sub>2</sub> as an initiator. The mixture was heated to reflux for 2 – 10 hours. After the completion of the reaction, the solvent was removed by using a rotary evaporator followed by high vacuum distillation to isolate the product. The synthesis of O(4-VP) has been reported in previous work [20].

### 2.5 Synthesis of O(4-VP)

The synthesis was carried out by reacting 25 g O(4-VP) and platinum oxide (1-2 g) in 150 mL glacial acetic acid. The reaction was run for 24 hours at room temperature under 40-60 p.s.i. of hydrogen. After the completion of the reaction, the mixture was subjected to rotary evaporation to separate the product from the solvent, and the product was tested as corrosion inhibitor without further treatment.

### 2.6 Weight Loss Measurement

Weight loss measurement was commenced to investigate the efficacy of the synthesized inhibitors, with particular purpose to compare the performance of the inhibitors in brine solution without and with kerosene addition. For this purpose, two sets of experiments were carried out with 3 replications (triplicates). In the first set, test solution consists of brine solution only (without kerosene) and the second set consists of brine solution with kerosene. Each set was conducted to determine corrosion rate by weight loss measurements with and without corrosion inhibitor. In the first set, each of six test bottles was filled by 175 mL of brine solution, and three of them were added by inhibitor O(4-VPP) with concentration of 10 mg L<sup>-1</sup>. In the second set of the experiment, each of six samples made up 140 mL brine solution and 35 mL kerosene were treated similarly as in the first set. Initially the coupons were placed in test bottle and purged for 45 minutes with CO<sub>2</sub> gas (at about

250 mL min<sup>-1</sup>), and the test bottles were capped with crown seals and finally placed in a rotated wheel oven at 50 °C for 24 hours. After the completion of the experiments, the bottles were removed from the oven, and the coupons were removed and immediately placed in Clarke's solution (a solution composed of 2% of Sb<sub>2</sub>O<sub>3</sub> and 5% SnCl<sub>2</sub>, dissolved in concentrated HCl) for 45 seconds in order to remove the corrosion product from the surface. The coupon was dipped into water for about 5 seconds and into ethanol for another 5 seconds, and then dried and accurately weighed.

To calculate weight loss (*W*), corrosion rate (*CR*), and the inhibition efficiency (%*P*), the following equations were used.

$$W = W_{(i)} - W_{(f)} \quad (1)$$

$$CR = \frac{10. W.365}{A.D.t} \quad (2)$$

$$\%P = \frac{(CR_o - CR_i)}{CR_o} \times 100\% \quad (3)$$

Where *W* = weight loss (gram), *W*<sub>(i)</sub> = initial weight, *W*<sub>(f)</sub> = end weight, *CR* = corrosion rate (mm<sup>-1</sup> = millimeter per year), *A* = area of coupon (cm<sup>2</sup>), *D* = density of metal (g cm<sup>-3</sup>), equal to 7.86 g cm<sup>-3</sup> for carbon steel, *t* = time of exposure (days), %*P* = persen protection, *CR*<sub>o</sub> = corrosion rate without inhibitor and *CR*<sub>i</sub> = corrosion rate with inhibitor.

### 2.7. Electrochemical Measurements

Electrochemical measurements were carried out using the experimental set-up that has been used in previous studies [20, 27, 28] as shown in Figure 1, used for EIS and LP analyses.

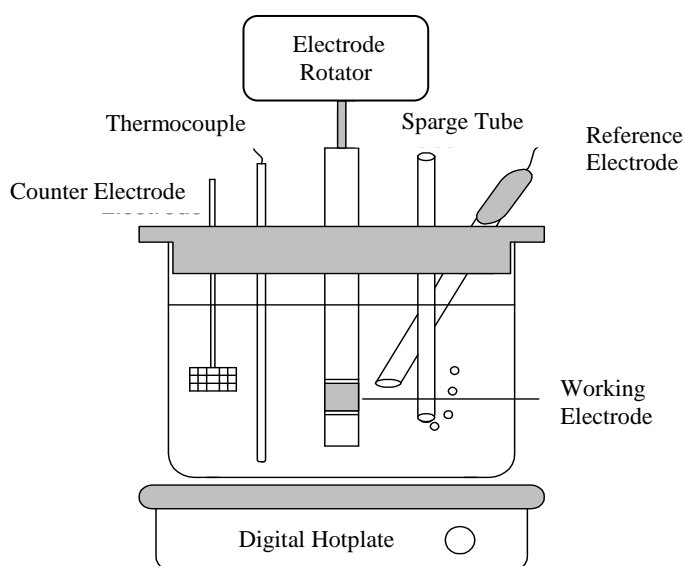


**Figure 1:** Cell assembly used for electrochemical measurements

To commence the experiment, the electrochemical cell (reaction vessel) was filled with 500 mL of brine solution and then saturated with CO<sub>2</sub> by purging the gas into the chamber for approximately 45 minutes. The purging with CO<sub>2</sub> at feeding rate of 100 mL min<sup>-1</sup> was maintained until the experiment was completed. The pH of the solution was found in the range of 4.0 – 5.0. The working electrode (sample) was assembled and fitted to the end of the threaded shaft that was connected to a Pine rotator. A platinum gauze auxiliary electrode, Ag/AgCl reference electrode, and thermocouple were placed in the cell, and then the cell was heated on a digital hot plate at specified temperatures of 30, 50, and 70 °C, regulated by a thermocouple. The working electrode was inserted and operated at a speed of 1000 rpm through connection to a Pine Model MSRX electrode rotator. The rotating electrode with speed of 1000 rpm was chosen for simulating turbulent flow conditions related to data obtained in real life system [28-30].

EIS measurements were performed using an EG&G Model 5210 Lock-in Amplifier and 273A Potentiostat controlled by EG&G Model 398 Electrochemical Impedance Software, Version 1.26. Impedance data were obtained using an AC voltage of 5 mV (RMS) over a frequency range of  $10^5 - 10^2$  Hz, with 8 points per decade. For linear polarization (LP) measurement, the electrochemical cell was connected to an EG&G Princeton Applied Research Model 273A Potentiostat and EG&G Model 314 Multiplexer, connected a computer equipped with EG&G Model 352 Corrosion Software, version 2.10 to control the process. The working electrode was polarized from +10 mV to -10 mV with respect to the corrosion potential using an anodic scan of  $0.1 \text{ mV s}^{-1}$ . This means that data collection was carried out every 200 seconds. The polarization resistance was determined from the ensuing potential current plot, and converted to a corrosion rate by using Tafel method assuming the slope of  $\beta_{ac} = 100 \text{ mV/decade}$ , which is the value specified for the instrument used for measurement, since Tafel measurement was not conducted. A blank measurement, with no inhibitor, was completed before inhibitor was added using a micro-pipette (0.1-0.2 mL). Eight LP measurements were completed for the blank and each inhibitor concentration, and last three readings were averaged to give a steady state corrosion rate. The experimental work was done at various temperatures. The inhibition efficiency (%P) was calculated by using Equation 3 [18,20] for LP data and Equation 4 [31] for EIS data:

$$\% P = \frac{(R_{ct(i)} - R_{ct(o)})}{R_{ct(i)}} \times 100\% \quad (4)$$

Where % P is inhibition efficiency in term of percent protection,  $R_{ct(i)}$  is charge transfer resistance with inhibitor and  $R_{ct(o)}$  is charge transfer resistance without inhibitor.

### 3. Results and Discussion

#### 3.1 Synthesis of Oligomers

Monomer (4-VP),  $\text{H}_2\text{O}_2$  and solvent, if combined in a suitable manner, will lead to polymerization.  $\text{H}_2\text{O}_2$  can be added to the solvent-monomer mixture, monomer may be added to solvent- $\text{H}_2\text{O}_2$  mixture and  $\text{H}_2\text{O}_2$  and monomer can be added to the solvent, or all can be changed simultaneously. A process for producing a linear PVP involved reacting one or more VP monomers in a solvent including alcohol and water in the presence of a catalytic amount of hydrogen peroxide, so as to polymerize the monomer or monomers to form the oligomer. As reported by Ilim et al [20] that product of oligomer 4-VP characterized by MALDI-TOF MS gives a molecular weight formula of:  $(105)n + 32 + 1$ , where 105 is the mass of repeating unit, n is the number of repeating units ( $n=2-22$ ), 32 is the combined mass of the end groups and 1 is the mass of one proton (attached during ionization). Using this formula, the clusters of peaks observed in the mass spectrum were correlated with their corresponding number of repeating units. The O(4-VP) was hydrogenated by using a platinum oxide catalyst, to produce oligomer 4-vinylpiperidine assigned as O(4-VPP). Furthermore, the oligomeric product synthesized was tested the efficacy as a carbon dioxide corrosion inhibitor.

#### 3.2 Weight Loss Measurement

Gravimetric method (weight loss) is a quantitative analysis relies on the process of weighing. This method is used to determine the corrosion rate and percent protection of inhibitor based on the calculation of the weight loss of the mild steel sample. The weight loss also known as wheel test was used as a screening method to evaluate the potential of corrosion inhibitor. The wheel test results carried out for the O(4-VPP) are shown in Table 1 and Figure 2.

The concentration of the inhibitor for weight loss experiments was fixed at  $10 \text{ mg L}^{-1}$ , since this experiment is basically carried out as a screening test, to justify whether the compound synthesized exhibits corrosion inhibition activity as expected. Experimental data in Table 1 represent the weight loss of the samples subjected to solutions with different compositions, and the weight loss values were calculated using Equation 1, and corrosion rate using Equation 2 with the results as compiled in Figure 2. Figure 2a represents the results in term of corrosion rate of the sample subjected to different experimental conditions. As can be seen, the use of inhibitor significantly decreased the corrosion rates, i.e. from  $3.35$  to  $1.25 \text{ mmy}^{-1}$  in the experiment without kerosene and from  $3.46$  to  $1.45 \text{ mmy}^{-1}$  in the experiment with kerosene. Percent protection was calculated from corrosion rate data using Equation 3, and the results are shown in Figure 2b. As can be seen in Figure 2b, kerosene promoted corrosion rates, resulted in lower protection offered by the inhibitor, in which the protection of  $62.7 \pm 9.9 \%$  was observed for the experiment without kerosene and reduced to  $58.1 \pm 1.6 \%$  for the experiment with kerosene addition. These results suggest that the ability of O(4-VPP) to protect the sample in medium containing kerosene is less than that in brine solution only. The effect of kerosene to reduce the inhibition

capacity of inhibitors has been reported by others using various inhibitors in different media [32,33]. To evaluate the both % protections, significant test was used. The significant test shows that the results of experimental  $t (t_{ex}) = 0.78$  and critical or table  $t (t_{0.95}) = 2.92$ . Based on the significant test, % protections of O(4-VPP) in brine solution with and without kerosene are not significantly different.

**Table 1:** Weight loss with the use of O(4-VPP)  $10 \text{ mg L}^{-1}$  in presence and absence of kerosene in rotated wheel oven at  $50^\circ\text{C}$  for 24 hours

No	Composition	Coupon dimension (cm)			A $\text{cm}^2$	Coupon weight (g)			CR $(\text{mm y}^{-1})$	Av CR $(\text{mm y}^{-1})$
		L	Wd	T		Wi	Wt	W		
1	B	2.017	1.043	0.119	4.936	1.9018	1.8678	0.034	3.20	
2	B	2.022	1.019	0.120	4.851	1.8704	1.8341	0.036	3.48	3.35±0.15
3	B	2.013	1.032	0.120	4.883	1.8766	1.8412	0.035	3.37	
4	B + K	2.013	1.036	0.120	4.903	1.9043	1.8684	0.036	3.40	
5	B + K	2.017	1.038	0.119	4.914	1.8953	1.8585	0.037	3.48	3.46±0.06
6	B + K	2.006	1.006	0.120	4.759	1.8313	1.7953	0.036	3.51	
7	B + I	2.023	0.980	0.121	4.692	1.7995	1.7888	0.011	1.06	
8	B + I	2.023	0.982	0.121	4.700	1.8008	1.7863	0.015	1.43	1.25±0.19
9	I + B	2.031	0.981	0.118	4.696	1.8239	-	-	-	
9	B + K + I	2.036	0.991	0.120	4.762	1.8342	1.8193	0.015	1.45	
10	B + K + I	1.965	1.016	0.121	4.714	1.8114	1.7970	0.014	1.42	1.45±0.03
11	B + K + I	1.996	1.016	0.120	4.779	1.8412	1.8260	0.015	1.48	

Note: B= brine solution, K= kerosene, I= inhibitor O(4-VPP)  $10 \text{ mg L}^{-1}$ , L= length, Wd= width, T= thickness, A=coupon area, Wi= initial weight, Wt= final weight, W= weight loss, CR= corrosion rate, Av CR= average corrosion rate

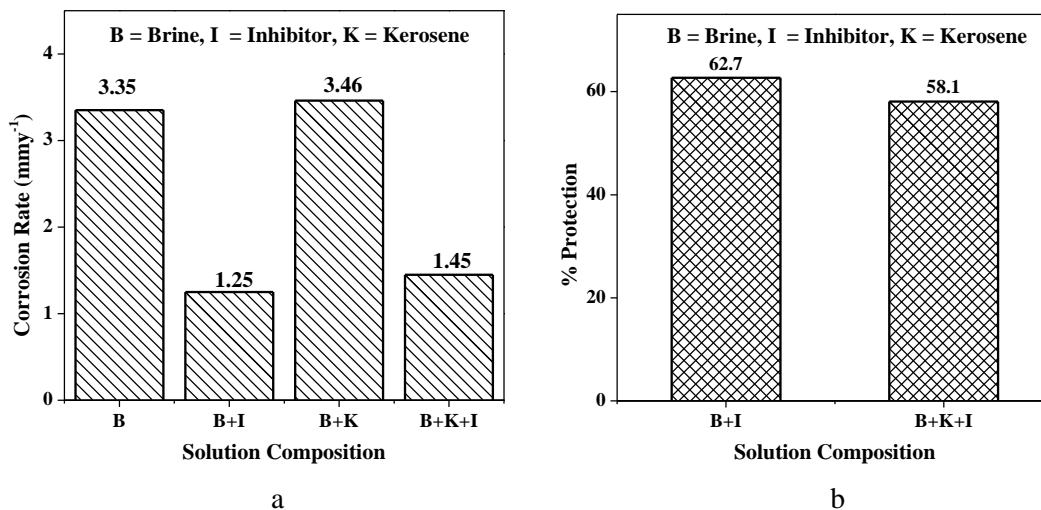


**Figure 2:** Corrosion rates (a) and % protections (b) of B (brine solution), B+I (brine solution + inhibitor), B+K (brine solution + kerosene) and B+K+I (brine solution+ kerosene + inhibitor) obtained by weight loss measurements in rotated wheel oven at  $50^\circ\text{C}$  for 24 hours

### 3.3 Electrochemical Measurement Results

Electrochemical measurements used in this research are electrochemical impedance spectroscopy (EIS) and linear polarization (LP). The EIS and LP experiments were conducted in-situ experiments, so mild steel samples (working electrodes) were immersed and data were collected during the experiments.

#### 3.3.1 EIS Results

Before running the experiments with O(4-VPP), a series of experiments was run with blank solution, *i.e.* brine solution saturated with  $\text{CO}_2$  gas, and tested for different temperatures of 30, 50, and  $70^\circ\text{C}$ , with the main purpose to evaluate the effect of temperatures on charge transfer resistance ( $R_{ct}$ ). The EIS data are presented as Nyquist plot, constructed by plotting the real impedance ( $Z_r$ ) against imaginary impedance ( $Z_i$ ), and the results obtained are presented in Figure 3.

The Nyquist plots obtained at open-circuit potential (OCP) in  $\sim -700$  mV indicated that there were only one time constant, and the system could be described by one-time constant model which consists of electrolyte resistance ( $R_s$ ), charge transfer resistance ( $R_{ct}$ ), and double layer capacitance as shown in Figure 4. Table 2 lists the circuit parameters which were obtained from the analysis of impedance spectra in Figure 3.

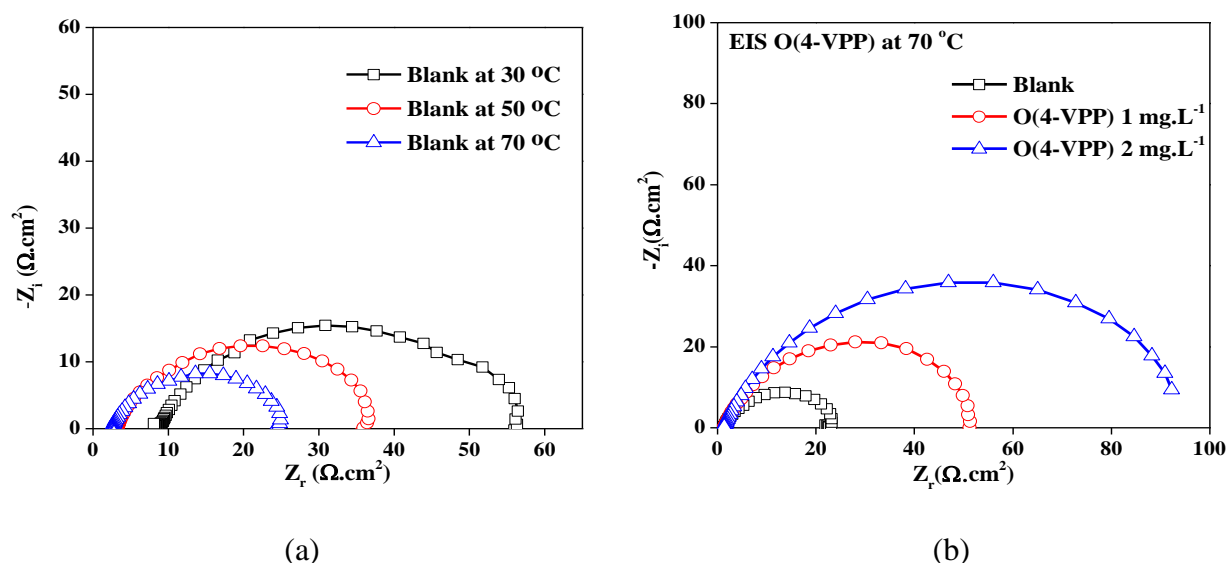


**Figure 3:** The Nyquist plots of (a) brine solution (blank) at 30, 50 and 70 °C and (b) blank and O(4-VPP) at various concentrations of 1 and 2 mg L<sup>-1</sup> at 70°C

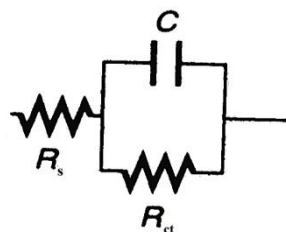


**Figure 4:** Equivalent circuit model used in the fitting of impedance data for the studied inhibitor

**Table 2:** Circuit parameters which were obtained from the analysis of impedance spectra in Figure 3 and % protections of O(4-VPP)

Composition of solution	Temperature (°C)	$R_s$ ( $\Omega \text{ cm}^2$ )	$R_s + R_{ct}$ ( $\Omega \text{ cm}^2$ )	$R_{ct}$ ( $\Omega \text{ cm}^2$ )	% P
Blank	30	8.1	56.5	48.4	-
Blank	50	2.9	36.6	33.7	-
Blank	70	2.8	24.8	22.0	-
Blank	70	1.4	23.2	21.8	-
O(4-VPP) 1 mg L <sup>-1</sup>	70	1.4	51.3	49.9	56.3
O(4-VPP) 2 mg L <sup>-1</sup>	70	1.4	92.3	90.9	76.0

As can be seen, the results indicate very significant effect of temperatures on the corrosion rates in term of charge transfer resistance ( $R_{ct}$ ), in which the larger the  $R_{ct}$ , the lower the corrosion rate. In Figure 3a and Table 2, the  $R_{ct}$  for the experiment run at 30 °C is 48.4  $\Omega \text{ cm}^2$ , and decreases to 33.7  $\Omega \text{ cm}^2$  at 50 °C, and to 22.0  $\Omega \text{ cm}^2$  at 70 °C. As expected, the figure shows that the  $R_{ct}$  value of the solution at 30 °C is higher than those for 50 °C and 70°C, confirming that the corrosion rate increases with increasing temperature. Figure 3a also displays significantly higher electrolyte resistance ( $R_s$ ) obtained for the experiment conducted at 30 °C than those observed for the experiments at higher temperatures. The activity of the solution is low at lower temperature related to high the resistance ( $R_s$ ) and low the corrosion rate, while at higher temperature, the solution has high activity, low the  $R_s$  and high the corrosion rate.

As reported by previous researchers [33] that  $R_{ct}$  of brine solution at 70 °C was found 18 to 22  $\Omega \text{ cm}^2$ , indicating that the results obtained in this present study are in agreement with the results reported by others. In general, it can be seen that at low concentrations, the inhibitor has exhibited high protection, and therefore low

concentrations (0-2 mg L<sup>-1</sup>) were selected for EIS experiments. Taking the temperature at which the corrosion rate is the highest into consideration, the EIS measurements with the O(4-VPP) as corrosion inhibitor were carried out at 70 °C. The EIS measurements were carried out with two concentrations of the inhibitor (1 and 2 mg L<sup>-1</sup>), against the blank solution, which is the brine solution only. The Nyquist plots produced are presented in Figure 3b.

The results presented in Figure 3b and Table 2 demonstrated significant effect of inhibitor in decreasing the corrosion. As can be seen, the use of inhibitor led to significant increase of the R<sub>ct</sub> as compared to the R<sub>ct</sub> of the blank solution. In addition, the significant effect of concentration is also demonstrated by the results, in which with the use of 1 mg L<sup>-1</sup> of O(4-VPP) to brine solution, the charge transfer (R<sub>ct</sub>) increased sharply 21.8 to 49.9 Ω cm<sup>2</sup>, and with the use of 2 mg L<sup>-1</sup> inhibitor, the R<sub>ct</sub> increased to 90.9 Ω cm<sup>2</sup>. By using Equation (4), the ability of the O(4-VPP) to protect the sample was calculated in term of % protection, giving the value of 56.3 % with the use of 1 mg L<sup>-1</sup> inhibitor and 76.0 % with the use of 2 mg L<sup>-1</sup>. These results are in accordance with the results obtained using weight loss measurement as has been discussed.

### 3.3.2 LP Results

LP measurements were carried out using concentrations of O(4-VPP) ranging from 0 to 20 mg L<sup>-1</sup>, and the results obtained are presented in Figure 5. Figure 5a presents a plot of the corrosion rate as a function of O(4-VPP) concentration and Figure 5b presents a plot of percent protection as a function of O(4-VPP) concentration at various temperatures.

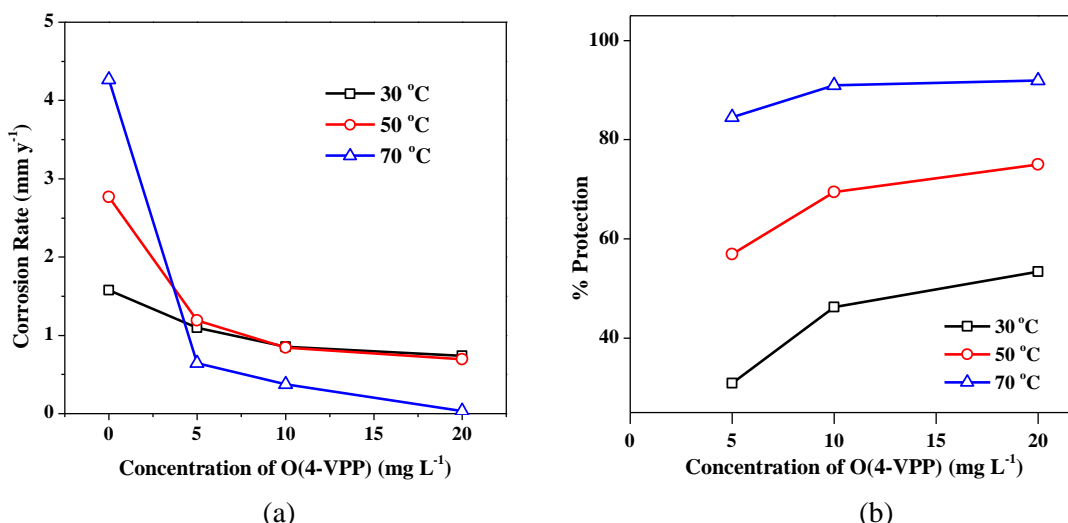


**Figure 5:** Corrosion rate (a) and % protection (b) of O(4-VPP) at various concentrations and temperatures

**Table 3:** The comparison result of % Protections of O(4-VPP) by using different methods

Method	Concentration (mg L <sup>-1</sup> )	Temperature (°C)	% P
Weight Loss	10	50	62.7
	1	70	56.3
EIS	2	70	76.0
	5	30	30.9
	10	30	46.3
LP	20	30	53.4
	5	50	56.9
	10	50	69.5
	20	50	75.0
	5	70	84.6
	10	70	91.0
	20	70	91.9

As shown in Figure 5(a), the use of inhibitor at concentration of 5 mg L<sup>-1</sup> resulted in obvious reduction of corrosion rate at the three temperatures applied. It was also found that addition of more inhibitor continued to reduce the corrosion rate of the samples, with the highest reduction was observed for the use of 20 mg L<sup>-1</sup>

inhibitor and the temperature of 70 °C. Based on the corrosion rate data in Figure 5a, the data showing effect of concentration at different temperatures on % protection are presented in Figure 5b, which indicate that the higher the concentration the better the protection. This LP results were compared by EIS and weight loss results as compiled in Table 3.

In addition, it can be seen that at the same concentration, the protection offered by the inhibitor is higher at higher temperature. This phenomenon suggests that the mechanism of inhibiting is a chemisorption rather than physisorption of the inhibitor on the surface of mild steel, as has been suggested by others [9,20,27,28]. Adsorption isotherms can be used to characterize the mechanism of adsorption of O(4-VPP) onto the mild steel surface as following explanation.

### 3.3.3 Adsorption Isotherm

The adsorption isotherms can study the nature of bond between the adsorbed inhibitor molecules and the metal surface. To characterize the mechanism of adsorption of O(4-VPP) onto the mild steel surface, surface coverage ( $\theta$ ) data obtained from LP measurements were used. The data were fitted to Temkin adsorption isotherm according to the Equation 5 [28] or Equation 6

$$K_{\text{ads}}C = e^{f\theta} \quad (5)$$

$$\ln C = f\theta - \ln K_{\text{ads}} \quad (6)$$

The molecular interaction constant ( $f$ ) can be obtained directly from the gradient of  $\ln C$  vs  $\theta$  and the log of adsorption equilibrium constant, ( $\ln K_{\text{ads}}$ ) is also obtainable from the intercept of the plots. The van't Hoff equation (Equation 7) was employed to calculate the enthalpy of adsorption, ( $\Delta H_{\text{ads}}$ ). To reduce errors in calculations, the surface coverage of 50% was used at various temperatures. The  $\Delta H_{\text{ads}}$  is calculated by the multiplication of the gradient of the van't Hoff plot by the gas constant ( $R$ ). The  $\Delta H_{\text{ads}}$  can be used in the calculation of other thermodynamic parameters, i.e., the free energy of adsorption ( $\Delta G_{\text{ads}}$ ) and the entropy of adsorption ( $\Delta S_{\text{ads}}$ ) by using Equation 8 and 9 [28].

$$\ln C = \frac{\Delta H_{\text{ads}}}{RT} + \text{constant} \quad (7)$$

$$\Delta G_{\text{ad}} = -RT \ln (K_{\text{ads}}) \quad (8)$$

$$\Delta S_{\text{ads}} = \frac{\Delta H_{\text{ads}} - \Delta G_{\text{ads}}}{T} \quad (9)$$

**Table 4:** Summary of thermodynamic parameters of adsorption for O(4-VPP)

Compound Name	T (°K)	$\ln K_{\text{ads}}$	$\Delta H_{\text{ads}}$ (kJmol <sup>-1</sup> )	$\Delta G_{\text{ads}}$ (kJmol <sup>-1</sup> )	$\Delta S_{\text{ads}}$ (JK <sup>-1</sup> )	$f$
O(4-VPP)	303	15.21		-38.30	195.64	3.97
	323	16.31	20.98	-43.79	200.53	8.08
	343	18.28		-52.13	213.15	8.06

Table 4 summarizes the thermodynamic data for O(4-VPP) by using Equation 6-9. The adsorption of O(4-VPP) on to the surface of mild steel is an endothermic process as shown by the positive enthalpy of adsorption and obviously thermodynamically spontaneous as shown by negative free energy of adsorption. In general, when the absolute value of  $\Delta G_{\text{ads}}$  is 40 kJ mol<sup>-1</sup> or larger, the adsorption of inhibitor on the sample surface is related to chemisorption [9,31,34]. Durnie et al [28] proposed that chemisorption process may be involved a net positive entropy of adsorption. The magnitude of  $f$  is related to the forces of Coulomb and Born repulsion factors arising from the interaction of adsorbing and neighboring adsorbed molecules that related to the charge at the hydrophilic head group of a molecule as well as steric effects, i.e., length, flexibility or branching of the hydrophobic chain and the size of the hydrophilic head group. A higher molecular interaction constant relates to stronger forces of repulsion between the adsorbed and adsorbing molecule [28]. Based on data obtained as shown at Table 4 and compared by previous researches, the adsorption of O(4-VPP) on the surface of mild steel



is attributable to chemisorption. The forces of repulsion between O(4-VPP) molecules adsorbed onto the surface of mild steel are higher at a higher temperature rather than at a lower temperature.

Regarding the inhibition mechanism by nitrogen containing inhibitor, Lopez et al. [35] proposed that the main contributor to the formation of metal-inhibitor bonds is most likely the pyridine-like nitrogen which acts as a strong base. In this respect, it is then concluded that the main contributor to the formation of metal-inhibitor bonds in O(4-VPP) synthesized in this study is nitrogen bound to piperidine moiety.

## Conclusions

In this study, the oligomer 4-vinylpiperidin, O(4-VPP) with the ability to protect mild steel against CO<sub>2</sub> corrosion was successfully synthesized from oligomer 4-vinylpyridin, O(4-VP). Corrosion experiments carried out demonstrated that the inhibitor offered protection in brine solution without and in the presence of kerosene, however better protection was observed in the absence of kerosene. The performance of the inhibitor in term of %-protection was found to be influenced by concentrations, in which the higher the concentration the higher the %-protection. The same is true for temperature, suggesting that the inhibitor was adsorbed onto surface of the mild steel through chemisorption. The chemisorption of the inhibitor by the surface of the sample is also supported by high agreement between the results of weight loss experiment, carried out with slow rotation, and the results of EIS and LP measurements conducted under strong stirring (1000 rpm)

## Acknowledgments

The authors wish to thank and appreciate the Directorate General of Higher Education (DIKTI), Ministry of Research Technology and Higher Education Republic of Indonesia for research funding provided through the Hibah Bersaing Research Grant Batch II, 2016, with Contract number: 144/SP2H/LT/DRPM/III/2016, 10 Maret 2016. One of authors, Ilim thanks to BPPDN for postgraduate scholarship.

## References

1. Shayegani M., Afshar A., Ghorbani M., Rahmaniyan M., *Corros. Eng. Sci. Technol.*, 43 (4) (2008) 290.
2. Nestic S., "Carbon Dioxide Corrosion of Mild Steel" in *Uhlig's Corrosion Handbook*, 3<sup>rd</sup> Ed., John Wiley & Sons, Inc., (2011) 229.
3. Zhang G., Chen C., Lu, M., Chai C., and Wu Y., *Mater. Chem. Phys.*, 105 (2-3) (2007) 331.
4. Nestic S., *Corros. Sci.*, 49 (12) 2007) 4308.
5. Groysman A., and Brodsky N., *Accred. Qual. Assur.*, 10 (2006) 537.
6. Belahcene B., Benmossat, A., Mansri, A., Doughmane M.Z., Bacetti A., Sadek K., *J. Mater. Environ. Sci.* 7(8) (2016) 2965.
7. Tourabe M., Nohair, K., Nyassi, A., Hammouti, B., Jama, C., Bentis, F., *J. Mater. Environ. Sci.* 5(4) (2014) 1133.
8. Sasri V.S., *Green Corrosion Inhibitors: Theory and Practice*, 1<sup>st</sup> Ed., John Wiley & Sons Inc., Canada, (2011) 310.
9. Mazumder M.A.J., Al-Muallem H.A., Faiz M., and Ali, S.A., *Corros. Sci.*, 87(2014) 187.
10. Olivares GZ., Gayosso M.J.H., Mendoza J.L.M. *Mater and Corr.* 58(6)( 2007) 427.
11. Okafor P.C. Lin, x, Zheng, Y.G., *Corros. Sci.* 51 (4) (2009) 761.
12. Liu J. Yu, W. Zhany, J. Hu, S. You L. Qiao, G. *App. Surf. Sc.* 256 (14) (2010) 4729.
13. Desimore M.P. Gordillon G. Simisan S.N. *Corros. Sci.* 53 (12) (2011) 4033.
14. Tan Y., Hinton, B. Forsyth M. *Annual Conference of the Australian Corrosion Association* (2012) 409.
15. Ibrahim T., Gomes E. Obot I.B, Kamis, M. Abou Zour M. *J. Adhe Sc. & Tech.* 30 (23) (2016) 2523.
16. Jevhmovie I. Singer M. Nestic S. Mishovie-Slanhovic V. *Mater. & Corr.* 67 (7) (2016) 756.
17. Zhao J. Duan, H. Jiang R. *Inter. J. of Elec. Sc.* 10 (3) (2015) 2716.
18. El-Lateef H.M.A., Abbasov V.M., Aliyeva L.I., Khalaf M.M., *Egyptian J. Petroleum* 24 (2015) 175
19. Rajeev P., Surendranathan A.O., Murthy Ch.S.N., *J. Mater. Environ. Sci.* 3(5) (2012) 856.
20. Ilim I., Jefferson A., Simanjuntak W., Jeannin M., Syah Y.M., Bundjali B., Buchari, *Indones. J. Chem.* 16(2) (2016) 198.
21. Annand R.R., Hurd R.M., and Hackerman N., *J. Electrochem. Soc.* 112 (1965) 144.
22. Khalifa O.R., Abdul Hamid I.A., Mochtar S.M., and Kassab A.A., *Asian J. Chem.* 5 (1993) 749.
23. El-Khair M.B.A., Mostafa B., Khalifa O.R., Abed-Hamid I.A., and Azzam A.M., *Corrosion Prevention Control*, 34 (1987) 152.

24. Abed Y., Arrar Z., Hammouti B., Aouniti A., Kertit S., and Mansri A., *J. Chem. Phys.* 96 (1999) 1347.
25. Abed Y., Arrar Z., Hammouti B., Taleb M., Kertit S., and Mansri A., *Anti-Corrosion Methods and Materials* 48(2001) 304.
26. Abed Y., Hammouti B., Touhami F., Aouniti A., Kertit S., Mansri A., Elkacemi K., *Bull. Electrochem.* 17 (2009) 105.
27. Durnie W.H., *Development of a Structure/activity relationship for carbon dioxide corrosion inhibitors, PhD Dissertation*, School of Applied Chemistry. Perth, Curtin University of Technology, (2000).
28. Durnie W.H., De Marco R., Kinsella B.J, and Jefferson A., *J. Electrochem. Soc.* 146 (1999) 1751.
29. Farelas F., and Ramirez A., *Int. J. Electrochem. Sci.*, 5 (2010) 797.
30. Galvan-Martinez R., Mendoza-Flores J., Duran-Romero R., and Genesca J., *Material Corrosion*, 58 (2007) 514.
31. Zhang H.H., Pang, X., Zhou, M., Liu, C., Wei, L., Gao, K., *App. Surf. Sci.* 356 (2015) 63.
32. Leon L.D.L., Rodriguez, M.A.V., Cruz, V.E.R., Calderon, F.A., and Garcia, S.A.P., *Int. J. Electrochem. Sci.* 6(2011) 3497.
33. De Marco R., Durnie W., Jefferson A., Kinsella B., and Crawford, A., *Corrosion* 58(4) (2002) 354.
34. De Souza F.S., Giacomelli C., Goncalves R.S., Spinelli A., *Materials Sci. and Engineering C* 32 (2012) 2436.
35. Lopez D.A., Simison S.N., and de Sanchez S.R., *Electrochim. Acta* 48 (2003) 845.

(2017) ; <http://www.jmaterenvironsci.com>